A coupled model study on the Atlantic Meridional Overturning Circulation under extreme atmospheric CO_2 conditions

Rita Lecci[1,*], Simona Masina[2,3], Annalisa Cherchi[2,3], Marcelo Barreiro[4]

[1] *Fondazione Centro Euro-Mediterraneo sui Cambiamenti Climatici, Lecce, Italy*

[2] *Fondazione Centro Euro-Mediterraneo sui Cambiamenti Climatici, Bologna, Italy*

[3] *Istituto Nazionale di Geofisica e Vulcanologia, Sezione di Bologna, Italy*

[4] *Universidad de la República, Facultad de Ciencias, Montevideo, Uruguay*

Article history
Received September 10, 2014; accepted May 5, 2016.
Subject classification:
Atlantic Meridional Overturning Circulation (AMOC), CO_2, Ocean stratification, Vertical diffusivity.

ABSTRACT

This study investigates the climate sensitivity to a strong CO_2 atmospheric forcing focusing on the North Atlantic Ocean (NA). The analysis is based on a set of 600 years long experiments performed with a state-of-the-art coupled general circulation model (CGCM) with the 1990 reference value of atmospheric CO_2 multiplied by 4, 8 and 16. Extreme increases in atmospheric CO_2 concentration have been applied to force the climate system towards stable states with different thermo-dynamical properties and analyze how the different resulting oceanic stratification and diffusion affect the Atlantic Meridional Overturning Circulation (AMOC). The AMOC weakens in response to the induced warming with distinctive features in the extreme case: a southward shift of convective sites and the formation of a density front at mid-latitudes. The analysis of the density fluxes reveals that NA loses density at high latitudes and gains it southward of 40 °N mainly due to the haline contribution. Our results indicate that the most important processes that control the AMOC are active in the high latitudes and are related to the stability of the water column. The increased ocean stratification stabilizes the ocean interior leading to a decreased vertical diffusivity, a reduction in the formation of deep water and a weaker circulation. In particular, the deep convection collapses mainly in the Labrador Sea as a consequence of the water column stratification under high latitudes freshening.

1. Introduction

The Atlantic Meridional Overturning Circulation (AMOC) has a major role in the Earth's climate system being responsible for one third of the northward global ocean heat transport [Ganachaud and Wunsch 2000]. Past abrupt climate changes are often explained in terms of oceanic heat transport associated with the AMOC [Rahmstorf 2002]. Nevertheless, the processes that control the response of the AMOC to external forcing, such as atmospheric CO_2 concentration, are not completely understood.

Several studies suggest that increased greenhouse gas (GHG) concentration may cause a reduction of heat loss and an enhanced freshwater input at high latitudes making the surface waters less dense in the northern sinking regions [Mikolajewicz and Voss 2000, Thorpe et al. 2001].

The Labrador Sea has been indicated as a susceptible region to increasing atmospheric CO_2 with changes in heat and freshwater fluxes contributing to the reduction of the water column density and the formation of deep waters southwest of Greenland [Mikolajewicz and Voss 2000, Weaver et al. 2007]. However, which among heat and freshwater fluxes mostly influence the density changes at high latitudes is still an issue of discussion.

The enhanced stratification resulting from high latitudes freshening leads to decreased diffusivity through the water column, since more turbulent kinetic energy is required to displace water parcels across a strong vertical density gradient [Gargett and Holloway 1984]. The vertical diffusivity in turn is strictly connected with the vertical overturning in the ocean interior [Welander 1986, Nilsson and Walin 2001, Nilsson et al. 2003, Marzeion et al. 2010]. A strongly stratified ocean shows a smaller vertical overturning when the total rate of small scale mixing energy supply (from winds and tides) is kept constant [Kuhlbrodt et al. 2007].

The location of ocean stratification that is most important in controlling the strength of the AMOC is still an open issue. While previous studies focused on the main role of low latitude mixing [Nilsson et al. 2003], Marzeion et al. [2007] showed that high latitude mix-

ing may be critical in controlling the vertical propagation of buoyancy anomalies imposed at the surface, and thereby it can influence stratification and circulation in the Nordic Seas. Thus, previous studies have shown that vertical diffusivity and stratification are potentially important factors controlling the AMOC behavior, and they may change under global warming conditions or under increased radiative and water fluxes forcing [Manabe and Stouffer 1994, Wood et al. 1999, Thorpe et al. 2001, Schmittner et al. 2005, Weaver et al. 2007, Marzeion et al. 2010].

In the present study we analyze the sensitivity of the AMOC to extreme atmospheric CO_2 concentrations in order to contribute to the understanding of the following still open questions:

- Which among heat and freshwater fluxes at high latitudes dominate the density field variations in response to a strong CO_2 forcing?

- What is the role of vertical diffusivity in response to the radiative forcing and where is it important?

To address these objectives, we performed a set of experiments consisting of a control simulation (CTRL) with a CO_2 concentration corresponding to the 1990 reference value and three simulations where that value is multiplied by a factor of 4, 8 and 16. Large changes in atmospheric CO_2 concentration have been applied in order to push the climate system to different stable states and analyze the main processes at the ocean surface and in its interior that control the response of the overturning circulation in the Atlantic. The idea that inspired these experiments is that when the system is forced to be far from its equilibrium state the feedback mechanisms at play may be highlighted. Sixteen times the present CO_2 atmospheric concentration is quite extreme but it has been found to present interesting nonlinearities in the simulation of the tropical climate [Cherchi et al. 2008, 2011].

All the experiments have been performed with a state of the art atmosphere-ocean-sea ice coupled general circulation model (CGCM) with a variable oceanic vertical diffusivity [Cherchi et al. 2008, Gualdi et al. 2008], which represent the most advantageous aspect of this study with respect to the previous ones that used oceanic circulation models with a simplified geometry [Nilsson and Walin 2001] and/or fixed vertical diffusivity or dependent on some powers of the stratification [Marzeion et al. 2007]. Furthermore, the model setup with atmosphere, ocean and sea-ice active components allows to compare the influence of high-latitude heat and freshwater fluxes on density changes.

The present study is organized as follows: Section 2 describes the model and the setup of the sensitivity experiments. In Section 3 the impact of the radiative forcing on the AMOC is discussed. Section 4 summarizes the response of the Atlantic Ocean mean state to the induced global warming, focusing in particular on the northern and southern sector. In Section 5 we analyze some possible mechanisms, like vertical water column diffusivity and stratification, influencing the simulated AMOC strength. Section 6 reports the main conclusions.

2. Model description and experiments setup

The SINTEX-G global coupled model [Gualdi et al. 2008] has been used to run experiments with modified CO_2 conditions, following previous studies by Cherchi et al. [2008]. SINTEX-G represents an improved version of the SINTEX model [Gualdi et al. 2003] with the inclusion of a module for interactive sea-ice [Fichefet and Morales Maqueda 1997, Timmermann et al. 2005]. Atmosphere, ocean and sea-ice are active, coupled components while land-ice is prescribed. The atmospheric and oceanic components are coupled with OASIS2.4 [Valcke et al. 2000].

The atmospheric component is Echam4.6 [Roeckner et al. 1996]. The resolution used in our simulations is a spectral T30 horizontal resolution with $3.75° \times 3.75°$ grid-points and 19 vertical sigma levels with the top level at 10hPa.

The oceanic component is OPA8.2 [Madec et al. 1998] used in ORCA2 configuration. It is a primitive equation model with a spatial resolution of $2° \times 2°$ and a refinement up to 0.5 degrees in the proximity of the Equator. Vertical resolution includes 31 vertical levels in z-coordinates with 14 levels lying in the top 150 meters and a free surface.

In the oceanic model parameterizations, the international equation of state of seawater [UNESCO 1981] has been used

$$\rho(S,T,P) = (\rho(S,T,0))/(1 - P/k(S,T,P)) \quad (1)$$

where the density is expressed in terms of salinity (S), temperature (T) and pressure (P). $k = 1/\beta$ is the bulk modulus and β the compressibility. The equation is valid for salinity ranging from 0 to 42 psu, temperature ranging from -2 to $40°$C and pressure ranging from 0 to 1000 bars. It can be applied to all oceanic waters that have a chemical composition of standard seawater. In water masses different in composition from standard seawater, the differences involve only very small errors [Lewis and Perkin 1978].

The vertical eddy diffusivity K_v is calculated from the vertical turbulent fluxes, using a TKE closure scheme [Blanke and Delecluse 1993]. According to TKE scheme, the vertical diffusivity is computed as

$$K_v = K_m / P_{rt} \quad (2)$$

where K_m is the vertical eddy viscosity coefficient that can be written as $K_m = C_k I_k \tilde{e}^{1/2}$ where $C_k = 0.1$ is a constant, I_k is the fraction of the solar irradiance at depth k and $\tilde{e} = 0.5\,(\tilde{u}'^2 + \tilde{v}'^2 + \tilde{w}'^2)$ is the definition of TKE where u ,v and w are defined as the zonal, meridional and vertical components of the water velocity, respectively. Into the TKE equation, they are written as mean value plus a fluctuation part $x = \tilde{X} + x'$.

P_{rt} is the Prandtl number that rules the amount of turbulent mixing of the potential density compared to the turbulent mixing momentum. It is defined in relation to the Richardson number as:

$$P_{rt} = Rg / Rf \quad (3)$$

where Rg is the gradient Richardson number and Rf is the flux Richardson number, also know as the mixing efficiency. Turbulent momentum transfer is more efficient than turbulent heat transfer when $P_{rt} > 1$ and *viceversa*. In the experiments the background vertical diffusivity is set to $1.e^{-5}$ m^2/s, the minimum value of TKE is $7.1e^{-5}$ m^2/s^2 and the background vertical viscosity is $0.1.e^{-5}$ m^2/s.

In the present study we compare a control experiment (CTRL) to a set of sensitivity experiments with increased atmospheric carbon dioxide concentration. In the CTRL the carbon dioxide concentration is 353 ppmV, corresponding to the 1990 mean value. It has been multiplied by a factor of 4, 8 and 16 to build $4\times CO_2$, $8\times CO_2$ and $16\times CO_2$ experiments, respectively. Similar experiments as those considered here were analyzed by Cherchi et al. [2008, 2011] to study the impact of extreme CO_2 levels on the tropical climate.

In all the experiments, the oceanic initial conditions correspond to the mean climatology from Levitus temperature and salinity datasets [Levitus et al. 1998] and they are common to all the experiments. The CO_2 forcing has been applied at the beginning of each simulation and maintained for the whole length of the experiments. All the simulations are 600 years long. The applied forcing drives the system toward an equilibrium with different adjustment time depending on the forcing intensity. The net heat flux globally averaged at the ocean surface indicates very slow variations toward the end of each experiment indicating an almost stable climate (not shown). In the $16CO_2$ experiment, for example, the global mean net surface heat flux is subjected to considerable changes within the first 100 years (56% of reduction with respect to the initial value) and very slow variations during the last 100 years (4% of reduction). Similarly, the balance at the top of the atmosphere (TOA), computed as the sum of the TOA net shortwave and longwave radiation, indicates climate stability over the last 100 years of all CO_2

	CTRL	$4CO_2$	$8CO_2$	$16CO_2$
Global atm T	-	+7	+11	+17
Atlantic SST	-	+4	+7	+12
Atlantic SST gradient	27	26	25	24
Labrador SST	-	+3	+4	+8
Atlantic SSS	-	+1	+2	+4
Labrador SSS	-	-0.5	-1	-2
AMOC max	33	27	24	15
26 kg/m^3 Atlantic isopycnal depth	120	130	160	180
NA vertical diffusivity	1.6	1.2	0.9	0.4
SO wind stress	7.7	8	7.6	5.9
SO wind stress max	0.15	0.15	0.15	0.12
SO wind stress max lat	48°S	52°S	53°S	53°S
NA wind stress	3.5	3.6	3.5	2.4
NA wind stress max	0.10	0.11	0.11	0.08
NA wind stress max lat	48°N	51°N	52°N	53°N

Table 1. From top to bottom the values refer to annual mean differences (CO_2 experiments minus CTRL) of global 2 m height air temperature and of SST (°C) averaged in the Atlantic Ocean, annual mean meridional SST gradient in the North Atlantic (difference between 0° and 80°N), differences (CO_2 experiments minus CTRL) of SST (°C) averaged in the Labrador Sea and of SSS (psu) averaged in the Atlantic basin and in the Labrador Sea, annual mean AMOC maximum (Sv), depth (m) of the 26 kg/m^3 Atlantic isopycnal computed at the Equator, North Atlantic (60°N - 80°N) vertical diffusivity computed between 100-2000 m for boreal winter (10^{-4} m^2/s), Southern Ocean (30°S - 80°S) wind stress (10^{-2} N/m^2), Southern Ocean wind stress maximum (N/m^2) and latitude of the Southern Ocean wind stress maximum, North Atlantic (30°N - 90°N) wind stress (10^{-2} N/m^2), North Atlantic wind stress maximum (N/m^2) and latitude of the North Atlantic wind stress maximum.

simulations (not shown).

The SINTEX-G model performs generally well for climatological fields compared to observations as evaluated in many previous studies [Bellucci et al. 2008, Cherchi et al. 2008, 2012]. In particular, the CTRL experiment shows patterns of surface temperature, net heat flux and freshwater flux similar to observations and reanalyses [Cherchi et al. 2008, 2012]. However, a limitation of this coupled model is the prescription of the climatological river runoff. This deficiency has a negative impact on ocean salinity and leads the CTRL experiment to be 1psu overall saltier (not shown) than the Levitus 20th century climatology [Levitus et al. 1998]. This bias affects the ocean mean state. Even if the response of the ocean to the radiative forcing has been shown to depend on the mean state [Gregory et al. 2005], the analysis of the changes in the perturbed experiments still can provide information about the mechanisms that control the AMOC.

In the following sections, mean climate fields refer to the time average over the last 100 years of integration of each experiment, namely 500-600 years, unless otherwise specified. To simplify and quantify the description of the differences between perturbed and CTRL experiments, a number of Global or Atlantic mean parameters have been defined and summarized in Table 1.

3. Impact of increased atmospheric CO_2 forcing on the AMOC

The AMOC intensity is measured by the meridional overturning streamfunction. Its mean pattern computed for all the experiments is shown in Figure 1. The CTRL case shows the maximum value (33 Sv) at 1400 m depth (Figure 1a). The northward flow in the upper 1400 m transports warm and salty seawater to high latitudes where it cools and sinks to the deep ocean. The cold salty water then flows southward at 1500-4500 m depth.

The overturning cell shown by CTRL case is very strong compared to some existing estimates of the present climate AMOC strength from global ocean re-analyses (about 21 Sv) [Masina et al. 2011]. The enhanced formation of denser waters is a consequence of the prescription of climatological river runoff (see Section 2). At high latitudes dense waters can easily sink more vigorously reinforcing the AMOC strength [Bellucci et al. 2008] and affecting the mixed layer depth, which is generally deeper than observed [De Boyer Montegut et al. 2004]. Moreover, the AMOC deeps 1 km more than previous estimates that reported an AMOC maximum depth of 3000 m with the average depth of the maximum transport at 1000 m [Cunningham et al. 2007]. In CTRL experiment the AMOC fills all the Atlantic Ocean to the bottom not allowing the Antarctic Bottom Water (AABW) to enter

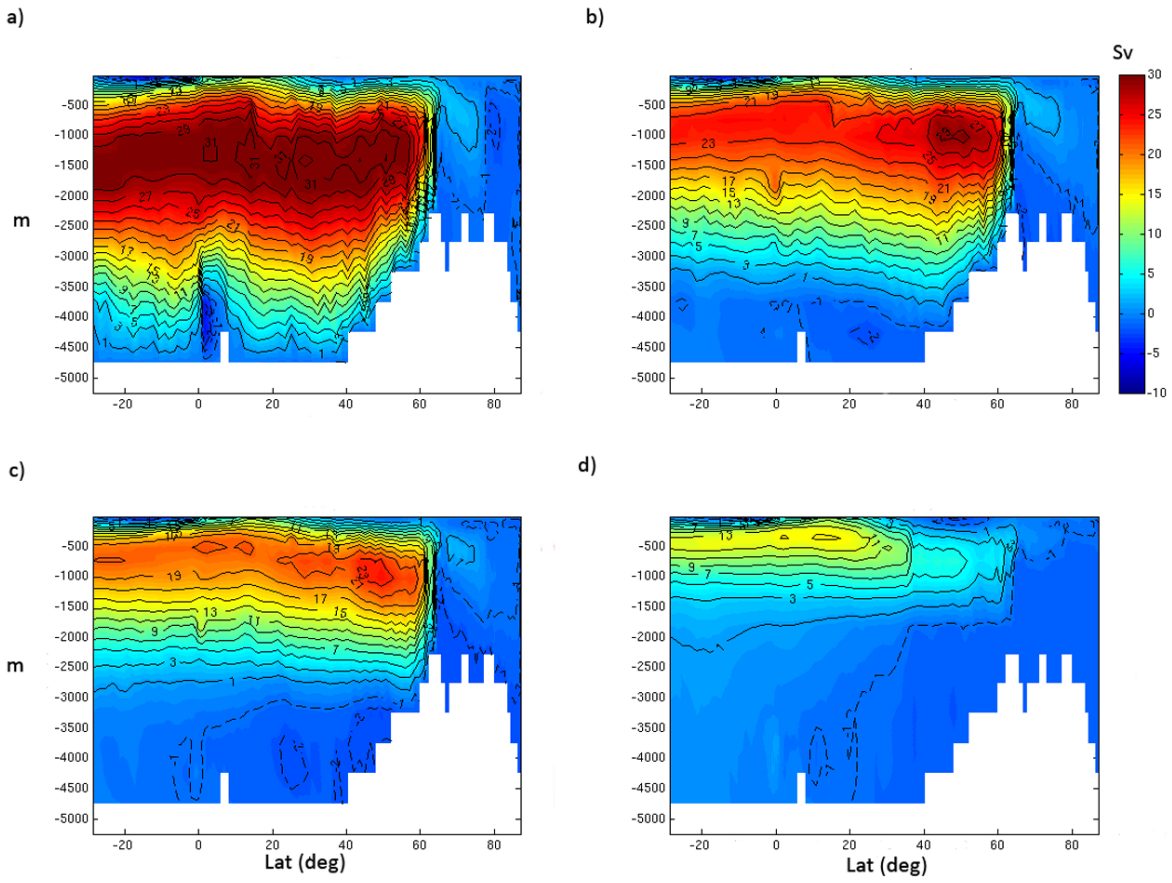

Figure 1. Annual mean meridional overturning streamfunction (Sv) for (a) CTRL, (b) $4CO_2$, (c) $8CO_2$ and (d) $16CO_2$ experiments.

into the basin and spread northward close to the ocean floor. Further, the AABW in our set of simulations do not form in the Weddell Sea but only in the Ross Sea spreading only into the Indo-Pacific Ocean (not shown).

In response to increased atmospheric CO_2 forcing, the entire AMOC cell weakens and becomes shallower (Figure 1b,c,d). The streamfunction maximum value lies between 30°N and 50°N in the CTRL, $4CO_2$ and $8CO_2$ experiments (Figure 1a,b,c, Table 1). On the other hand, in the $16CO_2$ experiment the maximum is located between the Equator and 20°N and the circulation north of 40°N weakens by about 27 Sv compared to the CTRL (Figure 1d).

The weakening of the meridional overturning circulation under increased CO_2 forcing is in agreement with several coupled model results [Dixon et al. 1999, Wood et al. 1999, Mikolajewicz and Voss 2000, Thorpe et al. 2001, Gregory et al. 2005, Schmittner et al. 2005, Weaver et al. 2007]. However, the magnitude of the AMOC weakening is highly model dependent with model climate sensitivity playing an important role: under atmospheric CO_2 forcing less sensitive models (e.g. CCSM4) show less AMOC weakening than more sensitive models (e.g. CESM1/CAM5) [Meehl et al. 2013]. Overall, on the basis of the models and range of scenarios considered, the IPCC Fifth Assessment Report (AR5) reports that it is very likely that the AMOC weakens because of global warming, but it is very unlikely that it collapses [Collins et al. 2013].

4. Induced Atlantic Ocean mean state and AMOC changes

4.1. South Atlantic

In response to the atmospheric CO_2 forcing, if the entire Atlantic sector is considered, the Arctic and the

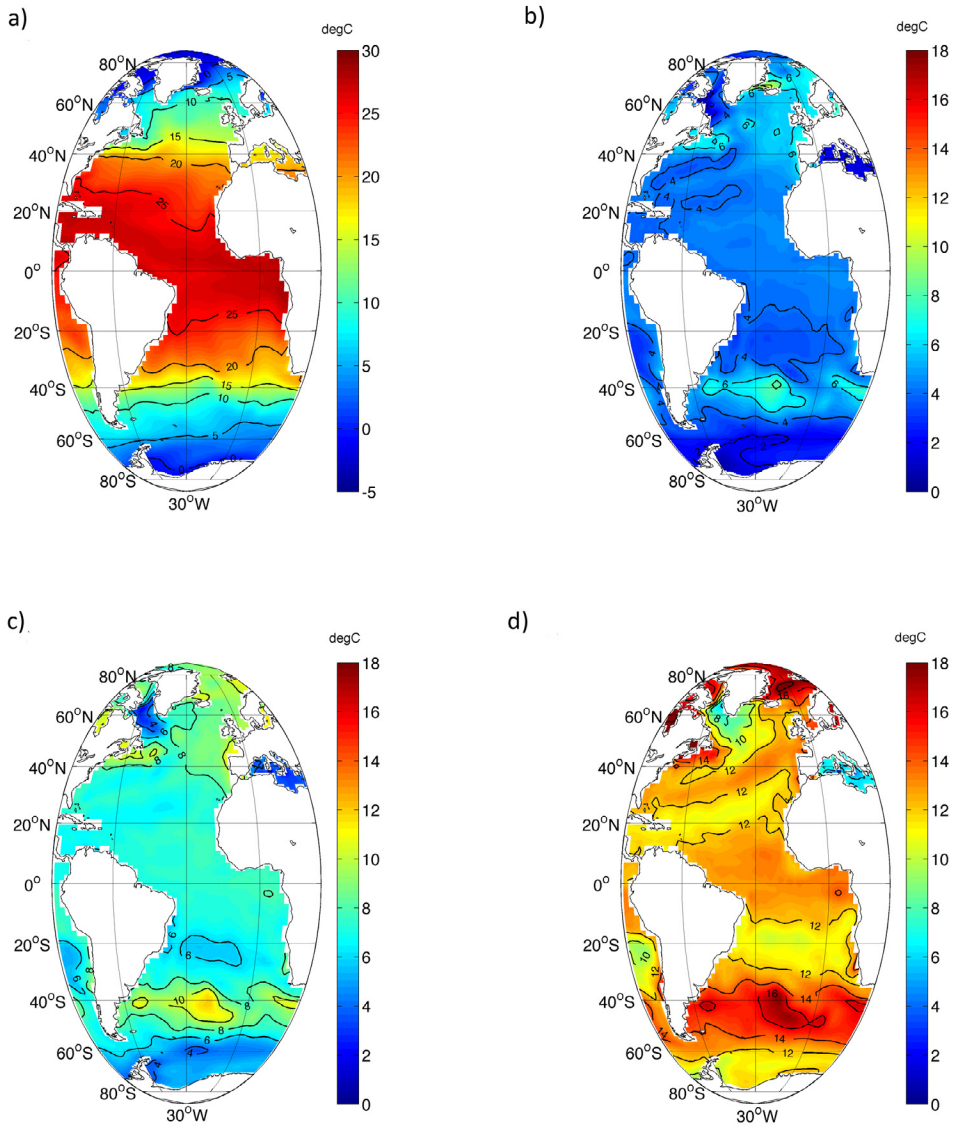

Figure 2. Annual mean SST (degC) for (a) CTRL experiment and differences between (b) $4CO_2$, (c) $8CO_2$ and (d) $16CO_2$ and the CTRL simulation.

South Atlantic experience the greatest warming. The annual mean sea surface temperature (SST) is shown in Figure 2. SST warms (Table 1) with the maximum increase located in a belt between 30°S and 50°S, consistent with a poleward shift of the subtropical gyre induced by a southward shift of the wind stress maximum over the Southern Ocean (Table 1). The result is in agreement with Cai et al. [2003] who proposed a similar mechanism under global warming conditions. An analysis of the Southern Ocean westerlies wind stress (Figure 3a) shows their poleward shift associated with changes in their strength: the westerly wind stress magnitude increases in $4CO_2$ and $8CO_2$ cases and decreases in the $16CO_2$ experiment. These results partly agree with those of Toggweiler [2009], who suggested a poleward shift and strengthening of the westerlies over the past 50 years and 17,000 years ago, at the end of the last ice age, in response to a warming tendency.

As shown by several studies [Toggweiler and Samuels 1995, Saenko and Weaver 2004, Gnanadesikan et al. 2007, Hirabara et al. 2007], increased Southern Ocean wind stresses, in particular in the Drake Passage region (55°S - 63°S) as reported by Klinger et al. [2003], should lead to a stronger Atlantic overturning circulation and *viceversa*. Our findings show instead an AMOC strength that is not sensitive to the strength of the wind stress anomalies at the Drake Passage for the two cases with a smaller radiative forcing (not shown). The lack of correlation between the AMOC strength and the westerly wind stress over the Drake Passage could be due to the ocean vertical diffusivity. As suggested by Sévellec and Fedorov [2011], if the North Atlantic Ocean vertical diffusivity is strong enough to sustain the maximum part of the overturning, the Atlantic MOC becomes less sensitive to the wind stress over the Southern Ocean. The model used for our analysis shows in the North Atlantic very high values of vertical diffusivity in the CTRL experiment if compared to the ones reported by Gnanadesikan [1999] for the observations.

The vertical diffusivity, computed in the Atlantic Ocean high latitudes (60°N - 80°N) as an average over the first 2000 m of the water column depth for the winter period (DJF), is close to $1.6*10^{-4}$ m^2/s for the CTRL case while the observed climatological mean value ranges from $0.10*10^{-4}$ m^2/s to $0.15*10^{-4}$ m^2/s [Gnanadesikan 1999]. The high vertical diffusivity at high latitudes in the CTRL simulation is associated to a very strong mixing through the water column and to an AMOC which shows a maximum value 7 Sv larger than the 20th century AMOC maximum mean value [Gnanadesikan 1999]. The ocean vertical diffusivity ranges from $1.6*10^{-4}$ m^2/s in CTRL experiment to $0.4*10^{-4}$ m^2/s in the $16CO_2$ case, meaning the 25% of its original value. The $16CO_2$ experiment shows then a decreased Atlantic overturning strength accompanied by a strong wind stress reduction over the Drake Passage. The theory according to the Drake Passage wind stress influences the AMOC intensity [Gnanadesikan 1999] might hold among the sensitivity simulations only in the $16CO_2$ experiment.

Furthermore, many studies have addressed the complex relationship between Southern and Atlantic

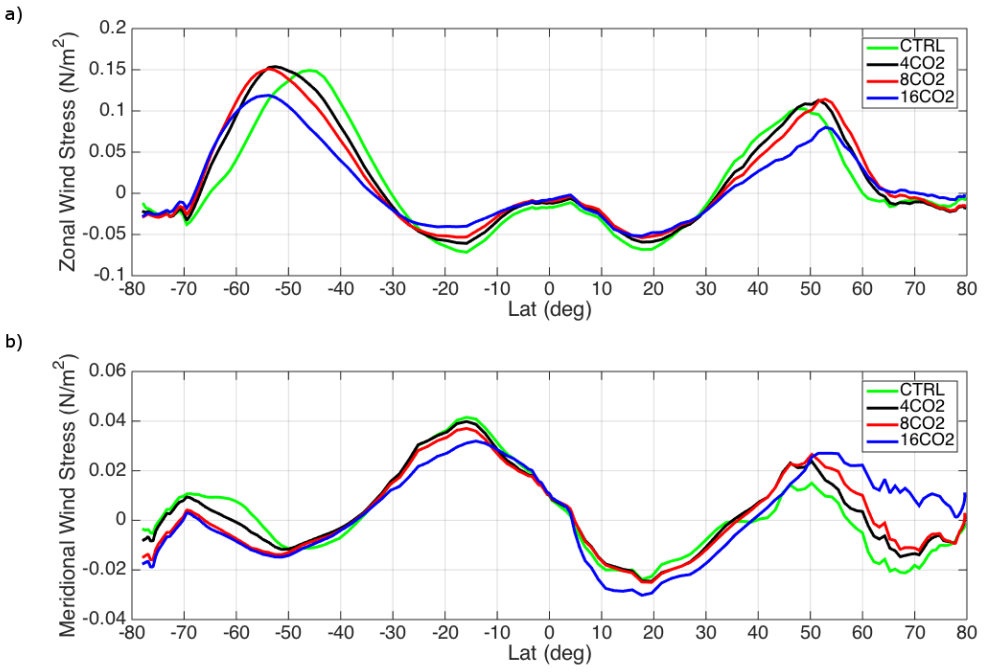

Figure 3. Annual mean intensity of (a) zonal and (b) meridional wind stress components (N/m^2) zonally averaged over the Atlantic Ocean for CTRL (green), $4CO_2$ (black), $8CO_2$ (red) and $16CO_2$ (blue) experiments.

Ocean circulation analyzing AABW transport and AMOC strength [Rahmstorf 2002, Hattermann and Levermann 2010]. It has been reported that reduction of deep-water formation in the North Atlantic generally leads to an intensification of AABW [Cox 1989, Stouffer et al. 2006]. Observations moreover show that, through water column mixing, AABW is the most important contributor to the lower branch of AMOC [Luyten et al. 1993] shifting it towards higher density as it moves southward in the South Atlantic [Reid 1989]. Even though our simulations have been performed with a global coupled model, the Atlantic Ocean does not show the AABW, making it impossible to analyze the effect of that deep circulation over the AMOC. Further, as mentioned above in our set of experiments the AABW do not form in the Weddell Sea but only in the Ross Sea spreading only into the Indo-Pacific Ocean (not shown).

4.2. North Atlantic

The induced warming influences also the North Atlantic leading to a decreased sea surface temperature gradient between low and high latitudes, computed as the SST difference between the Equator and 80°N (Table 1). The Labrador Sea shows a weaker temperature increase with respect to the North Atlantic Ocean: in $4CO_2$, $8CO_2$ and $16CO_2$ experiments the surface temperature is 2°C, 3°C and 6°C, respectively, lower than the North Atlantic warming (Figure 2b,c,d, Table 1). The anomalous behavior in the Labrador Sea simulated by the model could depend on changes in net heat fluxes (not shown); the ocean loses less heat with increasing CO_2 to the extent that in the extreme $16CO_2$ case the ocean gains heat from the atmosphere, instead of losing it as in the CTRL.

As for the SST field, the Labrador Sea SSS presents a peculiar behavior compared to the North Atlantic in

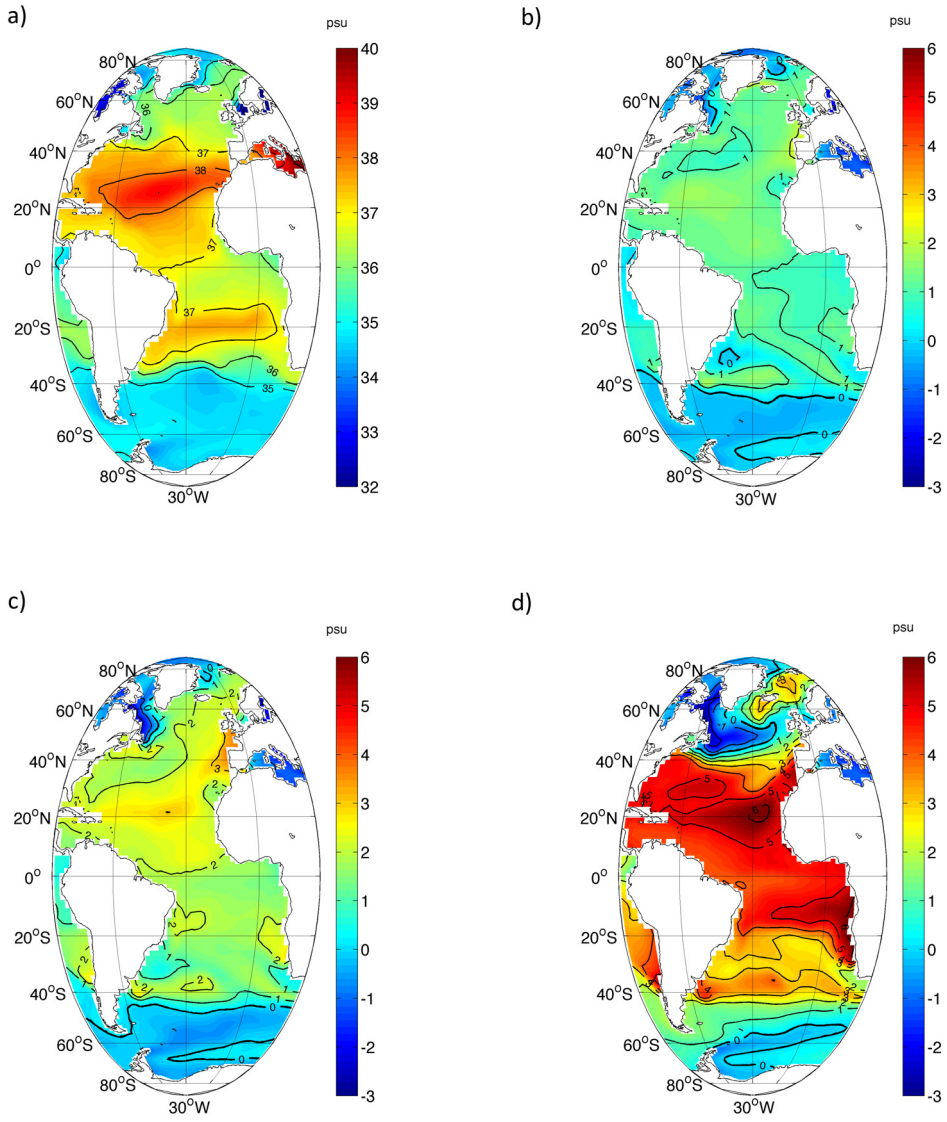

Figure 4. Annual mean SSS (psu) for (a) CTRL experiment and differences between (b) $4CO_2$, (c) $8CO_2$ and (d) $16CO_2$ and the CTRL simulation.

all CO_2 simulations, with a large SSS decrease with respect to the CTRL (Figure 4, Table 1). In the $4CO_2$ experiment there are SSS increases in the entire Atlantic basin with a maximum in the tropical North Atlantic in agreement with an early study of Manabe and Stouffer [1994]. The $8CO_2$ experiment shows a similar SSS pattern with increased intensity, except in the Labrador Sea area where there is a salinity front close to 40°N. This front is even clearer in the $16CO_2$ experiment (Figure 4d). The formation of the front results from a combination of increased meltwater and a changed Labrador current that allows fresh water to reach a lower latitude.

In the North Atlantic, in CTRL, $4CO_2$ and $8CO_2$ experiments the maximum current speeds are located along the Gulf Stream pathway (Figure 5a,b,c), but in the $16CO_2$ experiment they drastically weaken (Figure 5d). If compared to the CTRL, the Gulf Stream intensifies in the $4CO_2$ experiment, it remains almost unchanged in the $8CO_2$ experiment and it disappears in the $16CO_2$ (Figure 5). In the $16CO_2$ case, the large weakening of the westerlies's northward component causes the warm and salty surface tropical waters to stop at about 40°N allowing the Labrador Current to spread more southward (with respect to the CTRL), as it is no longer obstructed by the Gulf Stream. Hence a convergence zone is formed at mid-latitudes where tropical warm and salty surface waters meet cold and fresh Labrador Sea surface waters (Figure 5d). This behavior is consistent with the changes in North Atlantic (30°N - 90°N) wind stress (Figure 3, Table 1), as expected for a mainly wind-driven current. A decreased zonal stress together with an increased meridional stress let in $16CO_2$ experiment the total wind stress to push the surface waters more southward with respect to the CTRL experiment obstructing the northward flow of the Gulf Stream (Figure 5d). Many model studies, however, have shown a weakening of the Gulf Stream strength as response to a North Atlantic freshening induced by global warming and a larger dependence of the Gulf Stream intensity on the AMOC strength than on the surface wind changes [Greatbatch et al. 1991, Cai 1994].

The zonal-transport, influenced by wind-stress at

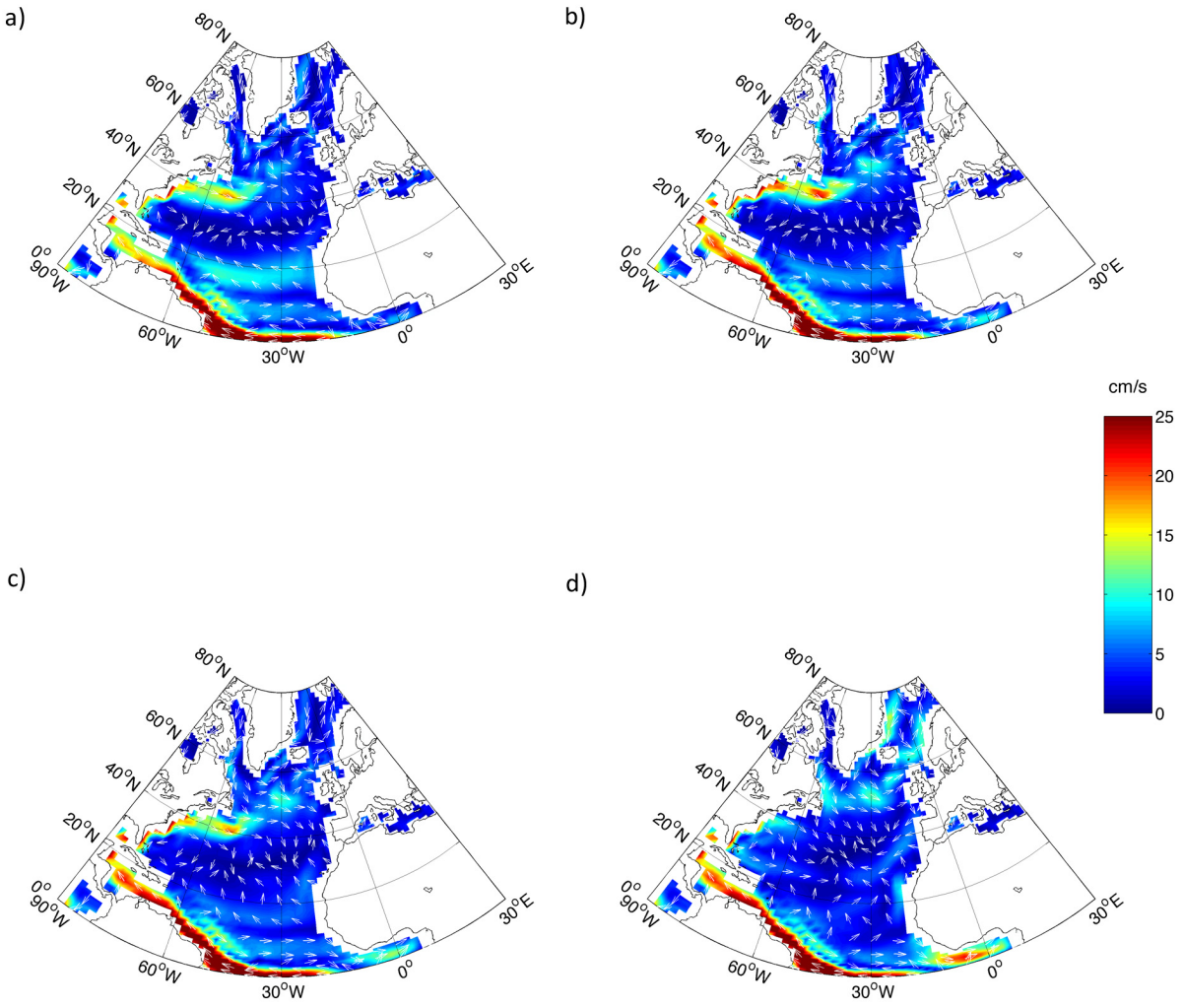

Figure 5. Annual mean surface currents (arrows give direction and shaded color the intensity in cm/s) computed for (a) CTRL (b) $4CO_2$, (c) $8CO_2$ and (d) $16CO_2$ experiments.

the sea surface, generally decreases in our experiments with increasing CO_2 atmospheric concentration. In particular, between 30°N - 40°N in $16CO_2$ experiment the transport decreases of about 1 Sv with respect to the CTRL. This result agrees with the weakening of zonal-wind stress in the North Atlantic whose intensity decreases from 0.04 N/m^2 in CTRL to 0.01 N/m^2 in $16CO_2$ experiment (Figure 3a). However, in $16CO_2$ experiment the zonal-transport enhances between 40°N - 50°N showing an increase of about 2 Sv with respect to the CTRL and reduces to almost zero between 50°N - 60°N (not shown). This behavior agrees with the density front formation at 50°N in response to the strongest radiative forcing applied. Due to the presence of the density front, the warm waters cannot spread more northward and mostly recirculate at mid-latitudes and the mainly wind-driven Gulf Stream tends to disappear (Figure 5d).

The pathway of the Gulf Stream has been shown to be strictly connected to the AMOC strength in many general circulation models, with a northerly (southerly) Gulf Stream path when the AMOC is strong (weak) [de Coetlogon et al. 2006]. In our set of simulations, due to the coarse resolution of the model used, it is very difficult to clearly establish the right dependency between Gulf Stream weakening and AMOC or wind stress changes. Further analysis should be performed with a higher resolution model in order to refine this analysis.

5. AMOC driving processes under extreme atmospheric CO_2 conditions

5.1. Changes in density field

The converge zone formed in the North Atlantic is evident in the sea surface density changes (Figure 6). In $4CO_2$ and $8CO_2$, as well as in CTRL, denser (lighter) waters are confined at high (low) latitudes, with a gen-

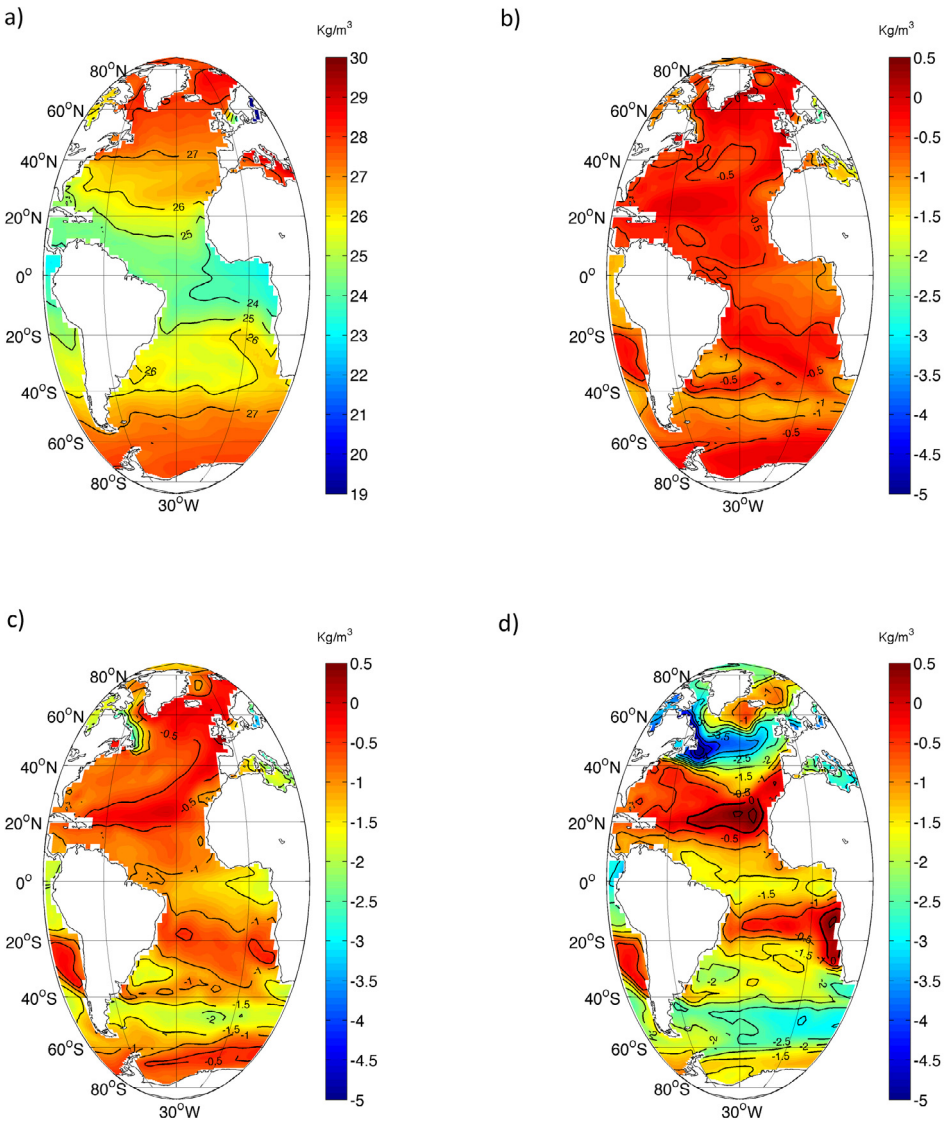

Figure 6. Annual mean surface density (kg/m^3) for (a) CTRL experiment and differences between (b) $4CO_2$, (c) $8CO_2$ and (d) $16CO_2$ and the CTRL simulation.

eral decrease of the density inside the basin as the carbon dioxide concentration increases in the atmosphere (Figure 6b,c). In $16CO_2$ experiment the density pattern shows a distinct front at 40°N with lighter waters (sigma density below 25 kg/m^3) northward and denser waters southward (Figure 6d). In high latitudes, changes in precipitation are larger than changes in evaporation (Figure 7) and this helps to decrease the surface water density, in addition to the contribution of freshwater input from northern latitudes sea-ice melting. In the present simulations the enhanced radiative forcing leads the Arctic sea-ice-cap to melt with different melting rates. The $4CO_2$ experiment shows a stabilization of Arctic sea ice volume after 86 years of simulation with a 99% volume reduction with respect to the CTRL. In the $8CO_2$ and $16CO_2$ experiments the Arctic is completely ice-free after 69 and 17 years of simulation, respectively (not shown). Thus, the sea ice melting releases freshwater at the rates of 0.01 Sv into 86 years, 0.02 Sv into 69 years and 0.06 Sv into 17 years in $4CO_2$, $8CO_2$ and $16CO_2$ experiments, respectively. The mentioned freshwater inputs have been obtained considering for each experiment the initial and final Arctic sea-ice cap volume, namely the volume loss, in relation to the elapsed time to reach a new stable sea-ice cap volume. This kind of experiments are similar to the highly idealized so-called water-hosing experiments where the North Atlantic freshwater balance is perturbed by artificially adding freshwater to the ocean basin. The aim of these experiments is to study the sensitivity of the AMOC to an external source of freshwater, mainly 0.1 Sv for 100 years, to the northern North Atlantic Ocean. In the water-hosing experiments, the input of water flux is switched off after 100 years of simulation and the experiment then continues without any further input of freshwater, in order to investigate whether or not the AMOC recovers its initial strength and the rate of the recovery [Stouffer et al. 2006]. It is important to note that in $4CO_2$ and $8CO_2$ experiments the freshwater input due to sea-ice melting is much smaller than the freshwater forcing used in the classical 0.1 Sv hosing experiments, while in the $16CO_2$ experiment is almost comparable being the 60% of 0.1 Sv.

To interpret the density changes and their influence on the AMOC strength, we have decomposed the density fluxes into haline and thermal components, following Large and Nurser [2001]. The results are shown in Figures 8 and 9 where the red (blue) color indicates a density gain (loss) with respect to the CTRL at the ocean surface. The North Atlantic loses density at high latitudes and gains density south of 40°N mainly due to

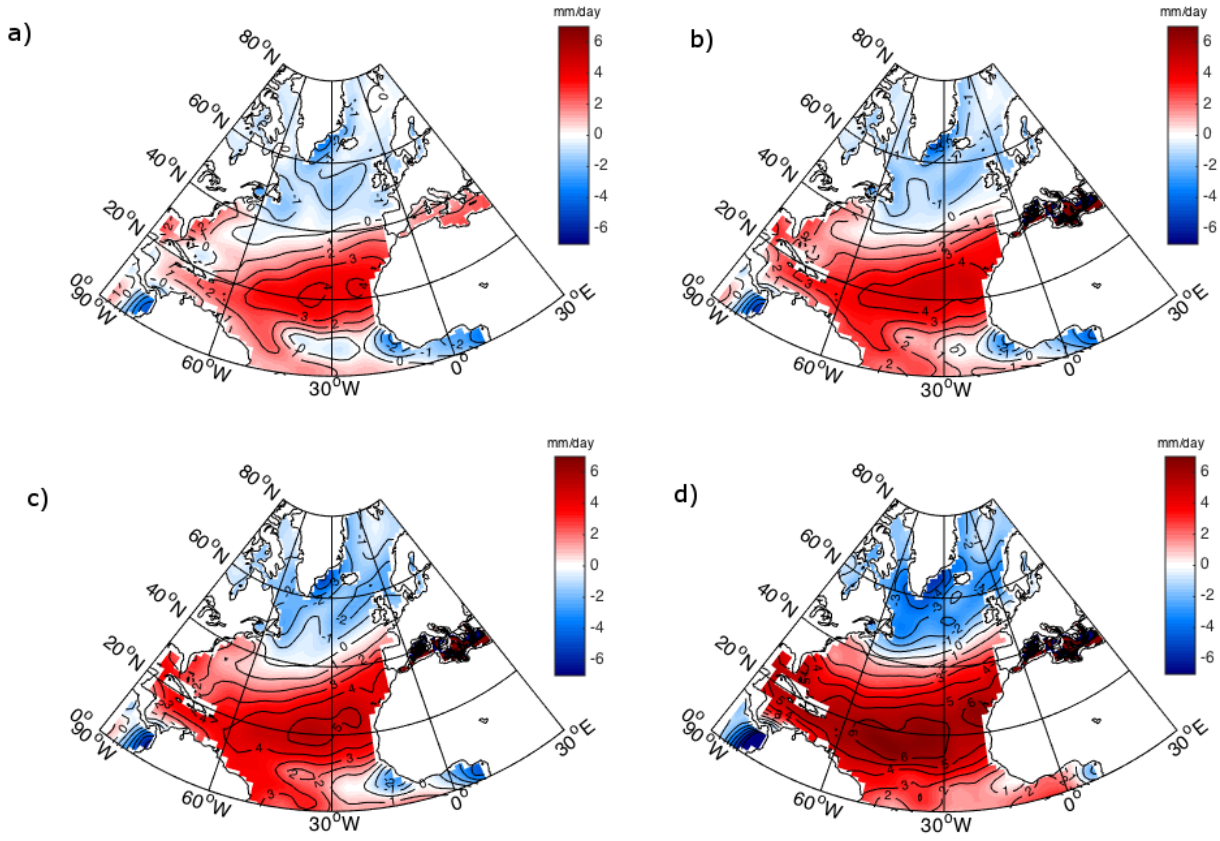

Figure 7. Annual mean freshwater fluxes (mm/day) computed for (a) CTRL, (b) $4CO_2$, (c) $8CO_2$ and (d) $16CO_2$ experiments.

the haline contribution (Figure 8), because of increased freshwater input (evaporation) at high (mid) latitudes. Cooling processes tend to increase the density in certain high latitude locations, but the thermal fluxes (Figure 9) are much weaker than the haline fluxes. In the CTRL experiment the largest thermal flux value is along the Gulf Stream pathway, which decreases in the perturbed experiments as CO_2 increases and the current itself weakens. In the $16CO_2$ experiment the thermal flux becomes negative in the Labrador Sea, further enhancing the density loss due to the freshwater input (Figure 9d).

As indicated by many studies [Mikolajewicz and Voss 2000, Weaver et al. 2007], the Labrador Sea is a region susceptible to increasing atmospheric CO_2. In that region, the changes in heat and freshwater fluxes contribute to the reduction of the water column density and the formation of deep waters southwest of Greenland.

Figure 10 shows annual mean density differences as latitude-depth sections in the Atlantic Ocean in the first 1000 meters. In the perturbed experiments the water column becomes lighter than in the CTRL mainly due to the strong warming (not shown), thus deepening the isopycnals (Table 1). In $16CO_2$, the density decrease at high latitudes is consistent with very little deep water formation north of 40°N, as indicated by the AMOC streamfunction changes (Figure 1d). In the Southern Hemisphere the large density decrease is linked to the weakening of Antarctic Intermediate Water (AAIW) that disappears in response to the strongest radiative forcing since the surface water is very warm and not dense enough to sink.

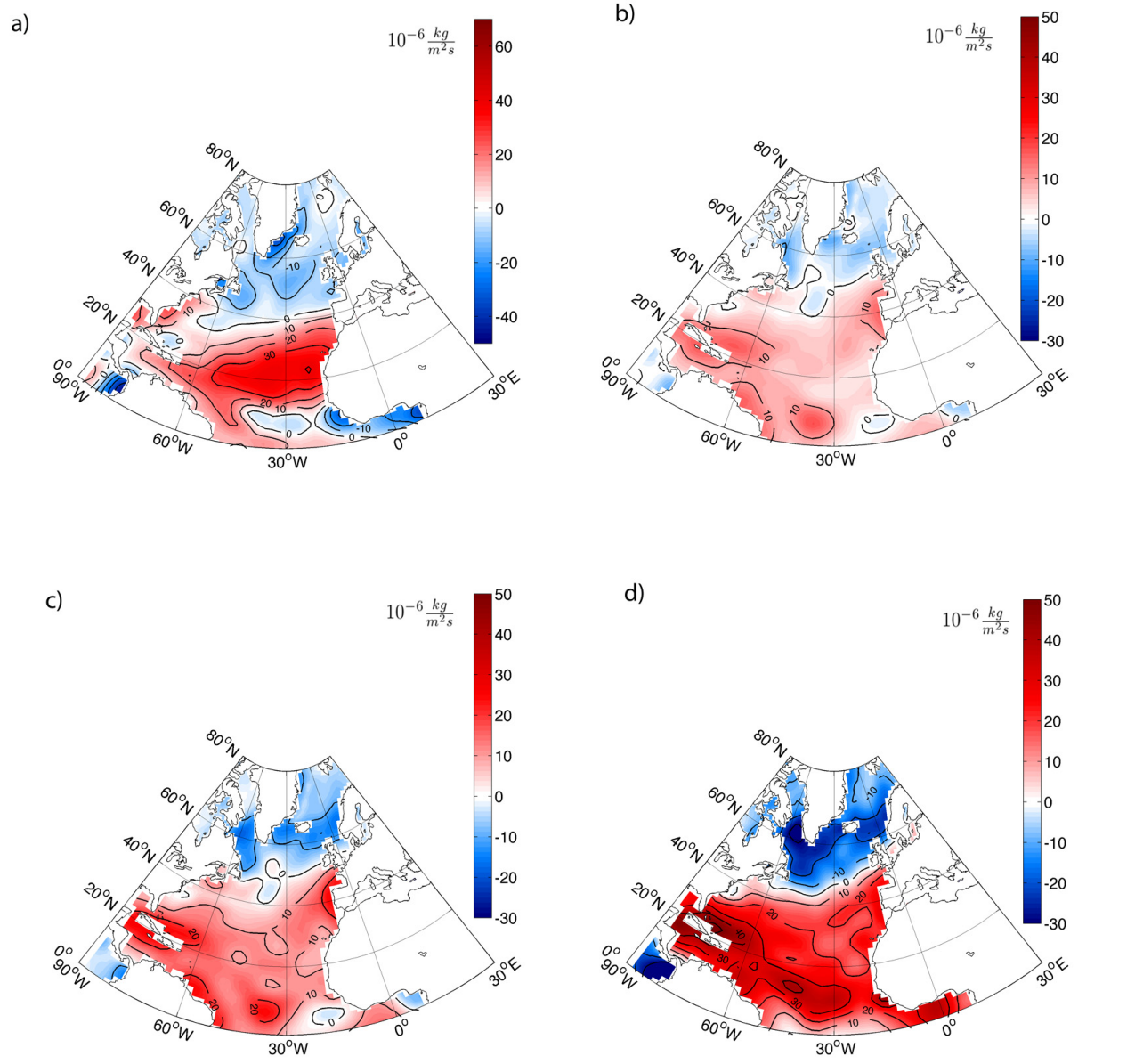

Figure 8. Annual mean haline density gain (10^{-6} kg/(m^{2}s)) computed for (a) CTRL experiment and differences between (b) $4CO_2$, (c) $8CO_2$ and (d) $16CO_2$ and the CTRL simulation.

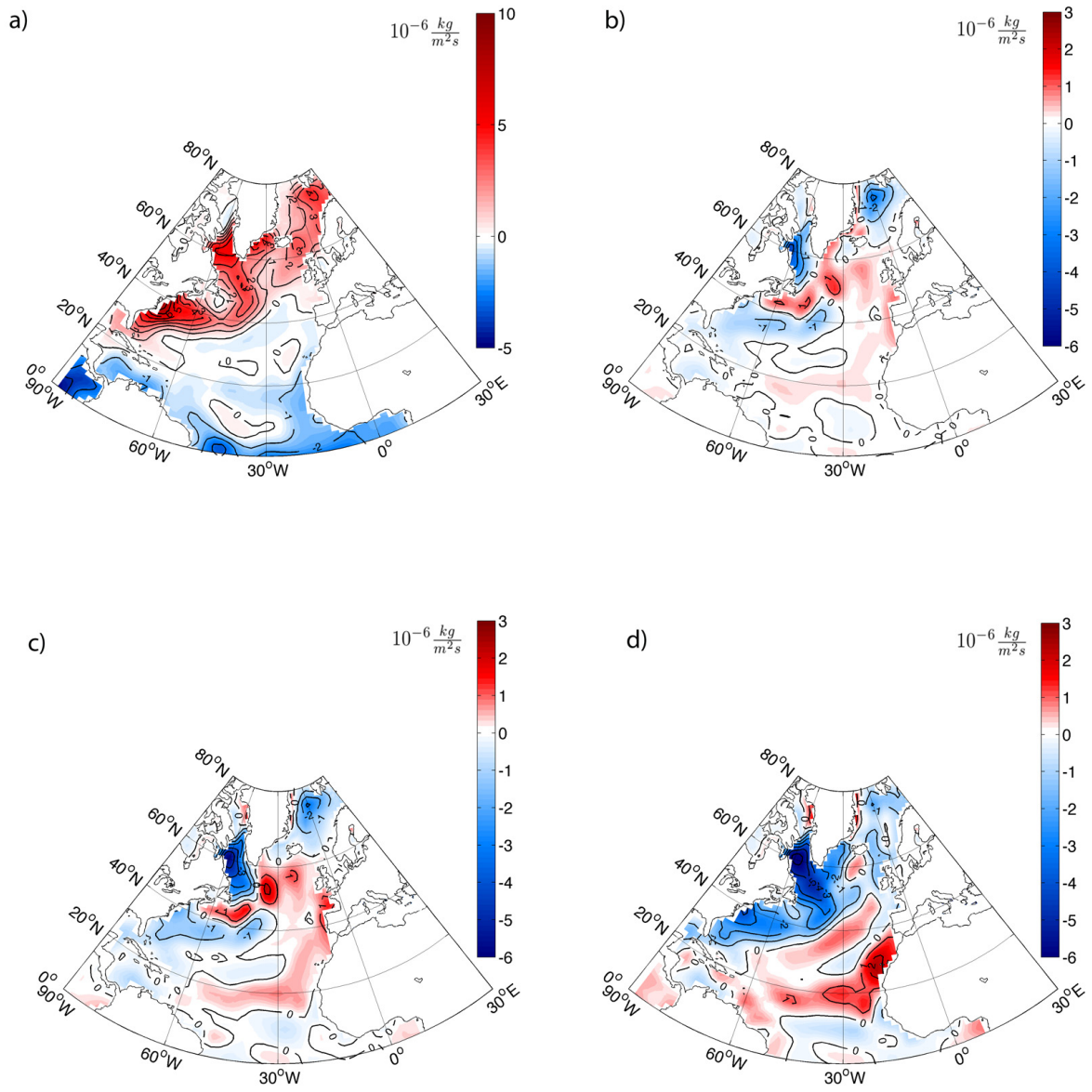

Figure 9. Annual mean thermal density gain (10^{-6} kg/(m^{2}s)) computed for (a) CTRL experiment and differences between (b) 4CO_2, (c) 8CO_2 and (d) 16CO_2 and the CTRL simulation.

5.2. North Atlantic stratification and AMOC strength

Changes in the AMOC structure are correlated with variations in the intensity and location of the deep-water formation, as shown by the spatial pattern of the winter (January - March) mixed layer depths in Figure 11. In the CTRL, deep convection occurs in the Nordic Seas, Irminger Sea and in the Labrador Sea (Figure 11a). As the radiative forcing increases, the mixed layer becomes shallower and convection weakens at all sites (Figure 11b,c,d). In particular, the 16CO_2 experiment shows a collapse of the strongest convective sites in the Nordic Seas and Labrador Sea and in the Irminger Sea maintains only one site (Figure 11d).

Wood et al. [1999] suggested that convection sites in the Labrador Sea and the Nordic Seas respond differently to global warming, showing in their 4CO_2 simulation a convection collapse in the Labrador Sea and a preservation of convection, or even reinforced, in the Nordic Seas. In the present study, the weakening of the AMOC with increasing CO_2 (Figure 1) is mainly the result of the shutdown of the convective sites in the Labrador Sea (Figure 11d). In the 16CO_2, the convective sites in the Nordic Seas (Figure 11d) are still active, although with a decreased intensity. In this case, most of the warm and salty tropical waters do not reach the high-latitudes, stopping instead close to 40°N and sinking there. Only a weakened branch of the Atlantic water flows further north and sinks in the Irminger Sea (Figure 1d).

Several studies reported the AMOC strength connected to vertical stratification and diffusivity into the ocean. Vertical diffusivity is strongly influenced by the vertical density stratification and Marzeion et al. [2007] have shown that, using a coupled climate model of intermediate complexity, if the ocean vertical stratification increases, the vertical diffusivity decreases leading to an AMOC weakening.

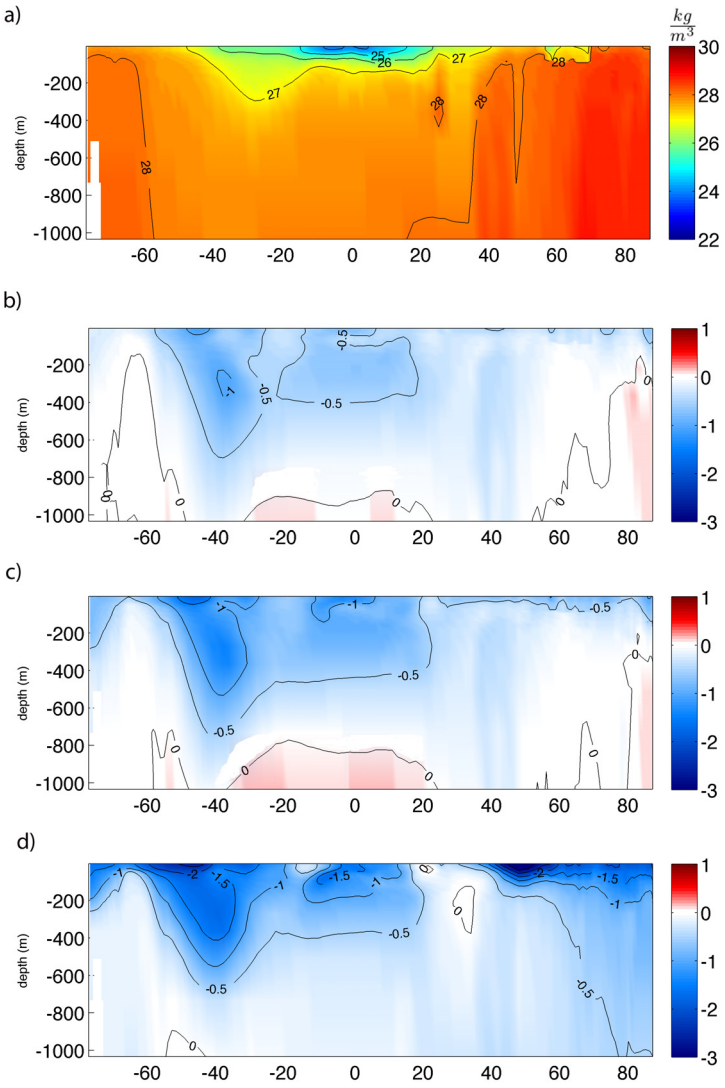

Figure 10. Zonally averaged vertical profile (0-1000 m) of annual mean density (kg/m^3) for (a) CTRL experiment and differences between (b) $4CO_2$, (c) $8CO_2$ and (d) $16CO_2$ and the CTRL simulation.

Figure 12 shows the correlation between stratification changes induced by the anomalous warming and freshening and the vertical diffusivity in the North Atlantic. Variations in water column stratification have been analyzed through the local buoyancy frequency defined as:

$$N = \sqrt{-\frac{g}{\rho_0}\frac{\partial \rho}{\partial z}} \qquad (4)$$

with g being the gravity acceleration, ρ_0 a reference density and $\frac{\partial \rho}{\partial z}$ the vertical density gradient. N has been computed as an annual mean around pycnocline depth (50 - 100 m) averaged over the Atlantic northern region 60°N - 80°N. Vertical diffusivity changes have been computed as the boreal winter climatological mean over the same latitudinal band and in the first 2000 m of water column. The season was chosen in order to consider the occurrence of the maximum overturning during the year and the depth level includes the location of its maximum. In our case, the ocean vertical diffusivity varies from 1.6e^{-4} m^2/s in CTRL to 0.4e^{-4} m^2/s in the $16CO_2$ case. The vertical diffusivity in the CTRL experiment (i.e. 1.6e^{-4} m^2/s) is much larger than the observed climatological values reported by Gnanadesikan [1999] ranging between 0.10e^{-4} and 0.15e^{-4} m^2/s. This large value at high latitudes in the CTRL is associated to a very strong mixing through the water column consistent with a very strong AMOC. Figure 12a evidences a strong negative linear relationship between winter mean vertical diffusivity and buoyancy frequency suggesting that an increased stratification in the convection sites over the North Atlantic (60°N - 80°N) is associated with reduction in the vertical diffusivity across the water column. This is in agreement with the increased water column stratification found mainly in the Labrador Sea as a consequence of changes in heat and freshwater fluxes. On the other hand, when computed at low latitudes (10°N - 30°N) and middle latitudes (30°N - 60°N) vertical diffusivity and water column stratification do not have any particular dependence upon each other (not shown).

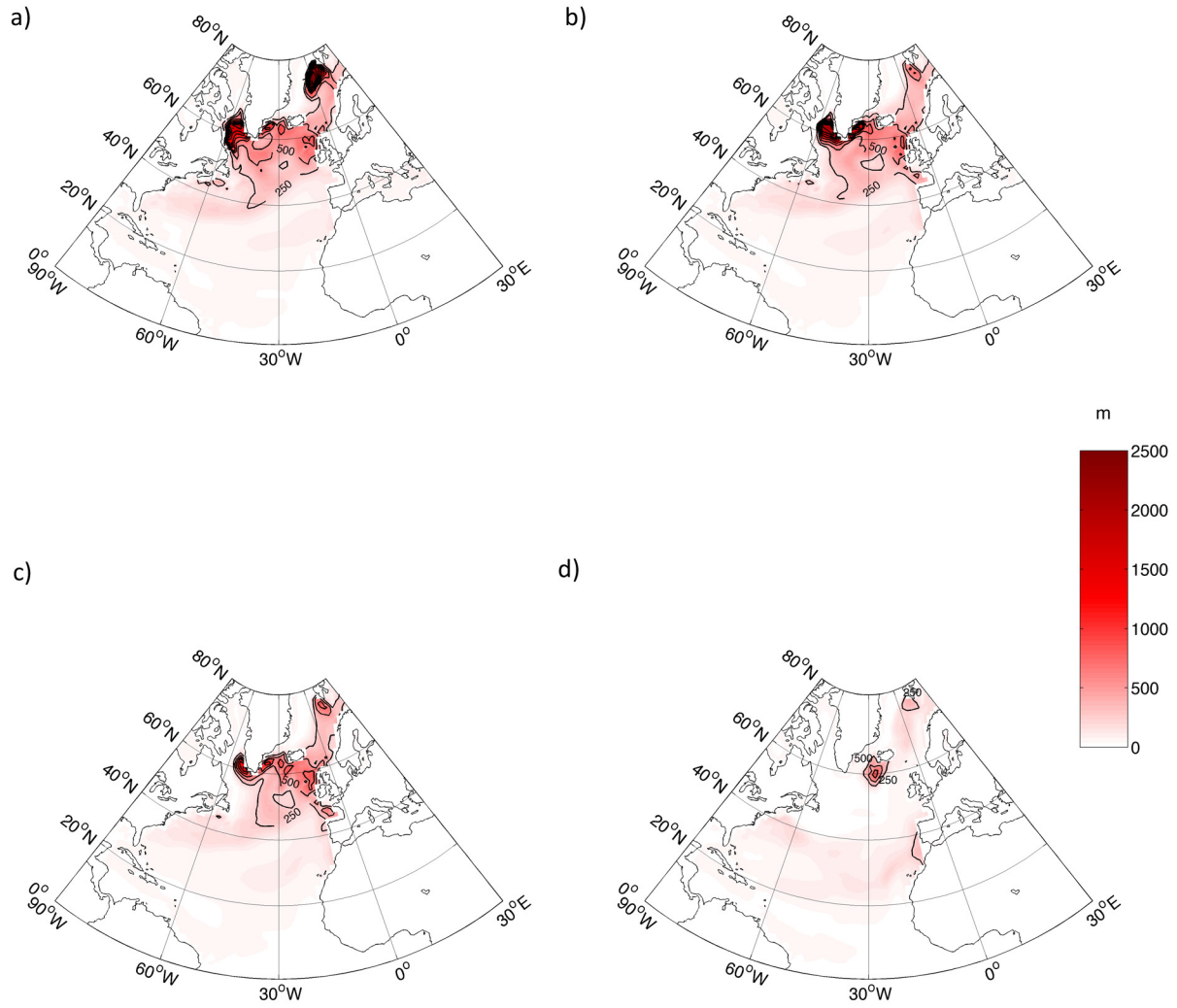

Figure 11. Mean winter (JFM) mixed layer depth (m) for (a) CTRL, (b) $4CO_2$, (c) $8CO_2$ and (d) $16CO_2$ experiments.

In our simulations, the mixing at high latitudes is the critical parameter that influences the circulation in the Nordic Seas. The vertical diffusivity shows the largest changes at high latitudes where it decreases by 31%, 44% and 75% in $4CO_2$, $8CO_2$ and $16CO_2$ experiments, respectively, in response to the radiative perturbation imposed (Figure 12b). When computed at low latitudes (10°N - 30°N), the vertical diffusivity slightly increases among the sensitivity experiments with a maximum increase in $16CO_2$ experiment (not shown). The increased vertical diffusivity at low latitudes can be associated with the increased thermal gradient through the water column since, in response to the global warming, the waters in the upper ocean become warmer while the water below become colder. The temperature difference between the ocean layers facilitates the turbulent diffusion movements through the water column increasing the vertical diffusivity.

The maximum streamfunction value at 25°N increases with vertical diffusivity (Figure 12b). The relationship holds as well when the vertical diffusivity is computed over 3000 m depth and for annual or summer climatology (not shown).

The positive linear relationship found between vertical diffusivity at high latitudes and the max AMOC strength implies that, as the vertical diffusion decreases with increased CO_2 forcing, so does the circulation intensity in the ocean basin. Our results are in close agreement with those of Bryan [1987] and Klinger et al. [2003]: in their experiments with an oceanic model with variable diffusivity, they found a similar AMOC strength with similar vertical diffusivities (e.g. $0.5e^{-4}$ m^2/s vertical diffusivity in correspondence to an AMOC intensity ranging from 9.2 Sv to 11.1 Sv). The vertical diffusivity computed at middle latitudes (30°N - 60°N), instead, does not show a consistent behavior in response to CO_2 forcing and it does not show any clear relationship with the AMOC intensity changes (not shown).

In summary, the increased stratification at high latitudes associated with a decreased vertical diffusivity leads to less dense water formation (mainly in the Labrador Sea) and to a reduced Atlantic overturning. In particular, the deep convection in the Labrador Sea collapses in response to the radiative forcing applied

since the water column stratifies under high latitudes freshening. Hence, the ocean interior equilibrates leading to decreased high-latitudes vertical diffusivity and to a decreased AMOC intensity with no formation of North Atlantic Deep Water. These results agree with Marzeion et al. [2007] who suggested a crucial role for mixing at high latitudes.

6. Discussion and conclusions

The present study examines the sensitivity of the Atlantic meridional overturning circulation to large CO_2 perturbations in order to gain insight in the physical processes that dominate the behavior of the mean meridional overturning circulation in the Atlantic basin.

Increased atmospheric CO_2 experiments are performed with a state-of-the-art coupled model with variable oceanic vertical diffusivity. Overall, all atmospheric CO_2 concentrations used lead to warmer global climate with a warmer and more saline Atlantic Ocean.

The analysis of the density fluxes shows that the North Atlantic loses density at high latitudes and gains density south of 40°N mainly due to the haline contribution. The high latitudes density decreases mainly through increased freshwater input due to sea-ice melting and the extreme case ($16CO_2$) shows a strong weakening of the AMOC (up to 27 Sv north of 40°N). In all the experiments, density changes lead to an increased stratification of the Labrador Sea that reduces deep-water formation. In the extreme case the Labrador Sea water formation stops with a consequent reduction of the meridional circulation, in agreement with several CO_2 forcing studies [Stocker and Schmittner 1997, Gregory et al. 2005, Schmittner et al. 2005]. A limitation of this study, however, is the lack of freshwater input from land-ice melting and river runoff that could further influence the surface density changes.

The analyses we performed in our sensitivity experiments suggested a significant influence of the vertical diffusivity in the ocean interior on the AMOC strength and pointed out the crucial role of the vertical mixing at high latitudes, particularly in the Labrador Sea. In the area of deep-water formation a negative linear relationship has been found between the vertical diffusivity through the ocean interior and the water column density stratification: as the latter increases in response to the induced high latitudes freshening, the first decreases. Furthermore, at high latitudes a positive linear relationship is present in all the CO_2 experiments between the circulation intensity and the North Atlantic vertical diffusion: when the forcing applied increases, the vertical mixing through the water column decreases, in response to vertical density stratification, and the AMOC weakens.

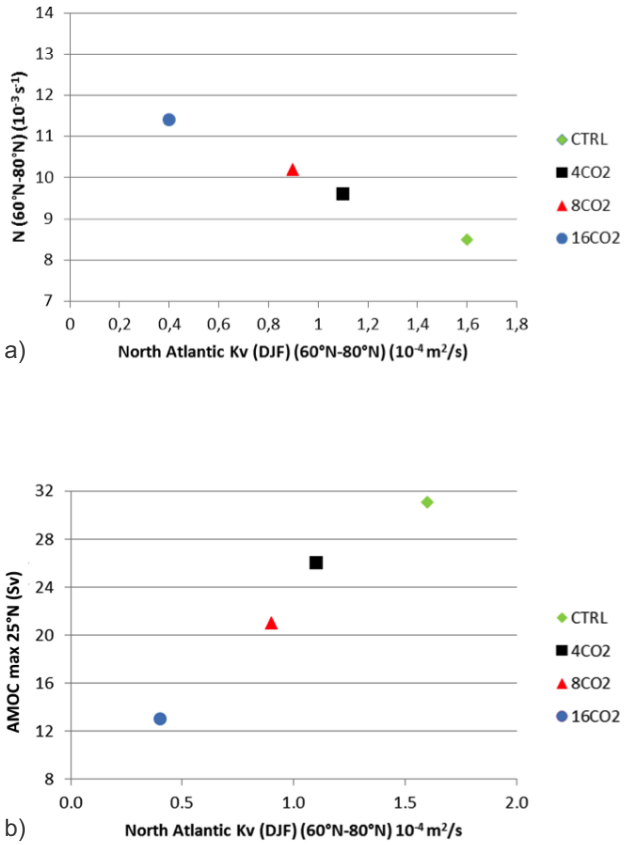

Figure 12. North Atlantic (averaged between 60°N - 80°N) winter mean vertical diffusivity (10^{-4} m^2/s) integrated between 100-2000 m depth, (a) *versus* buoyancy frequency N (10^{-3} s^{-1}) around pycnocline depth (i.e. between 50 and 100 m) and (b) *versus* AMOC max intensity computed at 25°N for CTRL (green diamond), $4CO_2$ (black square), $8CO_2$ (red triangle) and $16CO_2$ (blue circle) experiments.

When computed at low and middle latitudes, the vertical diffusivity does not show a clear dependence on the water column stratification and AMOC intensity changes. This result is in agreement with Marzeion et al. [2007] that found, using a model with vertical diffusivity proportional to some power of the stratification, a key role for mixing in high latitudes. Although the parameterization of vertical diffusivity used in our analysis is different from the one used by Marzeion et al. [2007], the results obtained are comparable since the water column stratification at high latitudes, responsible for the decreased vertical diffusivity in the ocean interior, depends on the same process: changes in the density field caused by changes in heat and freshwater fluxes.

On the other hand, our results contradict the one obtained by Nilsson and Walin [2001] and Nilsson et al. [2003] which showed, using an oceanic circulation model with a simplified geometry, a weakened stratification at high latitudes as consequence of an increased freshwater flux into the North Atlantic and related to an increased overturning. The uncoupled model used by Nilsson et al. [2003] shows instead an increase of the

stratification at pycnocline depth and in the deep ocean at low latitudes. As suggested by Marzeion et al. [2007], in the uncoupled model used by Nilsson et al. [2003] the changes in low-latitude diffusivity might be stronger than at high latitudes decreasing the AMOC strength by weakening the upwelling branch.

The mixing parameterization used in this study could be understood as an approximation to a better representation of vertical mixing in the ocean. Our results indicate that there may exist a feedback between stratification and vertical mixing that may be powerful enough to substantially increase the sensitivity of the AMOC to freshwater forcing caused by an increased radiative forcing. In the experiments presented, it is the amplification of a positive stratification anomaly in high latitudes that is causing the strongly nonlinear response of the system. In previous studies, it was a similar positive feedback amplifying a negative anomaly of the stratification in low latitudes.

An important difference of our study with that of Nilsson et al. [2003] is the use of a global ocean. As suggested by Marotzke and Klinger [2000], discussing the effect of stratification-dependent mixing in only one hemisphere may be insufficient to predict the behavior of a cross-equatorial overturning.

However, we should point out some limitations of this study. First, the use of a coupled model with relatively low ocean resolution may over-represent the importance of diffusive processes compared to those in the real ocean [Barreiro et al. 2008]. This results in a relatively more important role of the deep circulation compared to that of the shallow circulation in the ventilated thermocline and might affect the way in which the ocean adjusts to the forcing. Moreover, the freshwater input due to land-ice melting and river runoff changes, not considered in the present study, could further affect our results acting over the high latitude water column stratification and hence over the ocean vertical diffusivity. An even larger AMOC weakening should be expected in the CO_2 simulations if these processes were to be taken into account. Furthermore, even though our simulations have been performed with a global coupled model, as in Nilsson and Walin [2001] and Nilsson et al. [2003] the Atlantic Ocean does not show the AABW, leading to the impossibility of analyzing the effect of that deep circulation over the AMOC. Previous studies reported that a reduction of deep-water formation in the North Atlantic generally leads to an intensification of AABW [Cox 1989, Stouffer et al. 2006]. From observations it has been shown that through mixing, AABW is the most important contributor to the lower branch of AMOC [Luyten et al. 1993] shifting it towards higher density as it moves southward in the South Atlantic [Reid 1989].

Acknowledgements. We gratefully acknowledge the support of Italian Ministry of Education, University and Research and Ministry for Environment, Land and Sea through the project GEMINA. We thank N. Pinardi and A. Bellucci for useful comments on the interpretation of the results. We also thank D. Iovino who read a preliminary draft of the paper helping to improve it and P. Di Pietro for his technical support in managing and analyzing data.

References

Barreiro, M., A. Fedorov, R. Pacanowski and S.G. Philander (2008). Abrupt climate changes: How freshening of the northern atlantic affects the thermohaline and wind-driven oceanic circulations, Annu. Rev. Earth Pl. Sc., *36*, 33-58.

Bellucci, A., S. Gualdi, E. Scoccimarro and A, Navarra (2008). NAO-ocean circulation interactions in a coupled general circulation model, Clim. Dynam., *31*, 759-777.

Blanke, B., and P. Delecluse (1993). Low frequency variability of the tropical Atlantic ocean simulated by a General Circulation Model with mixed-layer physics, J. Phys. Oceanogr., *23*, 1363-1388.

Bryan, F. (1987). Parameter sensitivity of primitive equation ocean general circulation models, J. Phys. Oceanogr., 17, 970-985.

Cai, W. (1994). Circulation driven by observed surface thermohaline fields in a coarse resolution ocean general circulation model, J. Geophys. Res., *99*, 163-181.

Cai, W., P.H. Whetton and D.J. Karoly (2003). The response of the Antarctic Oscillation to increasing and stabilized atmospheric CO_2, J. Climate, 16, 1525-1538.

Cherchi, A., S. Masina and A. Navarra (2008). Impact of extreme CO_2 levels on tropical climate: a CGCM study, Clim. Dynam., *31*, 743-758.

Cherchi, A., A. Alessandri, S. Masina and A. Navarra (2011). Effects of increased CO_2 levels on monsoons, Clim. Dynam., *37*, 83-101.

Cherchi, A., S. Masina and A. Navarra (2012). Tropical Pacific-North Pacific teleconnection in a coupled GCM: remote and local effects, Int. J. Climatol., *32*, 1640-1653.

Collins, M., R. Knutti, J. Arblaster, J.L. Dufresne, T. Fichefet, P. Friedlingstein, X. Gao, W.J. Gutowski, T. Johns, G. Krinner, M. Shongwe, C. Tebaldi, A.J. Weaver and M. Wehner (2013). Longterm Climate Change: Projections, Commitments and Irreversibility, In: T.F. Stocker, D. Qin, G.-K. Plattner, M. Tignor, S.K. Allen, J. Boschung, A. Nauels, Y. Xia, V. Bex and P.M. Midgley (eds.), Climate Change 2013: The Physical Science Basis. Contribution of Working Group I to the Fifth Assessment Report of the Intergovern-

mental Panel on Climate Change, Cambridge University Press, Cambridge, United Kingdom, and New York, NY, USA.

Cox, M.D. (1989). An idealized model of the World Ocean, Part I: The global-scale water masses, J. Phys. Oceanogr., 19, 1730-1752.

Cunningham, S.A., T. Kanzow, D. Rayner, M.O. Baringer, W.E. Johns, J. Marotzke, H.R. Longworth, E.M. Grant, J.J.M. Hirschi, L.M. Beal, C.S. Meinen and H.L. Bryden (2007). Temporal variability of the Atlantic Meridional Overturning Circulation at 26.5°N, Science, 317, 935; doi:2010.1126/science.1141304.

De Boyer Montegut, C., G. Madec, A.S. Fischer, A. Lazar and D. Iudicone (2004). Mixed layer depth over the global ocean: an examination of profile data and a profile based climatology, J. Geophys. Res., 109, C12003; doi:10.1029/2004JC002378.

de Coetlogon, G., C. Frankignoul, M. Bentsen, C. Delon, H. Haak, S. Masina and A. Pardaens (2006). Gulf Stream variability in five oceanic general circulation models, J. Phys. Oceanogr., 36, 2119-2135.

Dixon, K.W., T. Delworth, M. Spelman and R.J. Stouffer (1999). The influence of transient surface fluxes on North Atlantic overturning in a coupled GCM climate change experiment, Geophys. Res. Lett., 26, 2749-2752.

Fichefet, T., and M.A. Morales Maqueda (1997). Sensitivity of a global sea ice model to the treatment of ice thermodynamics and dynamics, J. Geophys. Res., 102, 12609-12646.

Ganachaud, A., and C. Wunsch (2000). Improved estimates of global ocean circulation, heat transport and mixing from hydrographic data, Nature, 408, 453-457.

Gargett, A.E., and G. Holloway (1984). Dissipation and diffusion by internal wave breaking, J. Mar. Res., 42, 15-27.

Gnanadesikan, A. (1999). A simple predictive model for the structure of the oceanic pycnocline, Science, 283, 2077-2079.

Gnanadesikan, A., A.M. De Boer and B.K. Mignone (2007). A simple theory of the pycnocline and overturning revisited, Geoph. Monog. Series, 173, 19-32.

Greatbatch, R.J., A.F. Fanning, A.D. Goulding and S. Levitus (1991). A diagnosis of interpentadal circulation changes in the North Atlantic, J. Geophys. Res., 96, 9-23.

Gregory, J.M., et al. (2005). A model intercomparison of changes in the Atlantic thermohaline circulation in response to increasing atmospheric CO_2 concentration, Geophys. Res. Lett., 32, L12703; doi:10.1029/2005GL023209.

Gualdi, S., E. Guilyardi, A. Navarra, S. Masina and P. Delecluse (2003). The interannual variability in the tropical Indian Ocean as simulated by a CGCM, Clim. Dynam., 20, 567-582.

Gualdi, S., E. Scoccimarro and A. Navarra (2008). Changes in the tropical cyclone activity due to global warming: results from a high-resolution coupled general circulation model, J. Climate, 21, 5204-5228.

Hattermann, T., and A. Levermann (2010). Response of Southern Ocean circulation to global warming may enhance basal ice shelf melting around Antarctica, Clim. Dynam., 35, 741-756.

Hirabara, M., H. Ishizaki and I. Ishikawa (2007). Effects of the wind stress over the southern ocean on the meridional overturning, J. Phys. Oceanogr., 37, 2114-2132.

Klinger, B., S. Drijfhout, J. Marotzke and J. Scott (2003). Sensitivity of basinwide meridional overturning to diapycnal diffusion and remote wind forcing in an idealized Atlantic Southern Ocean Geometry, J. Phys. Oceanogr., 249-266.

Kuhlbrodt, T., A. Griesel, M. Montoya, A. Levermann, M. Hofmann and S. Rahmstorf (2007). On the driving processes of the Atlantic meridional overturning circulation, Rev. Geophys., 45, RG2001; doi:10.1029/2004RG000166.

Large, W.G., and A.J. Nurser (2001). Ocean Surface Water Mass Transformation, In: G. Siedler, J. Church and J. Gould (eds.), Ocean Circulation and Climate, Academic Press, San Diego, 317-336.

Levitus, S., T. Boyer, M. Conkright, T. O'Brein, J. Antonov, C. Stephens, L. Stathoplos, D. Johnson and R. Gelfeld (1998). World Ocean Database 1998, vol 1: Introduction, NOAA Atlas NESDIS 18, US Gov Printing Office, Washington D.C., 346 p.

Lewis, E.L., and R.G. Perkin (1978). Salinity: its definition and calculation, J. Geophys. Res., 83 (C1), 466-478.

Luyten, J., M.S. McCarteny, H. Stommel, R. Dickson and E. Gmitrowicz (1993). On the sources of North Atlantic Deep Water, J. Phys. Oceanogr., 23, 1885-1892.

Madec, G., P. Delecluse, I. Imbard and C. Levy (1998). OPA version 8.1 Ocean general circulation model reference manual, Note du Pôle de modélisation, Inst. Pierre-Simon Laplace (IPSL), France, No. 11, 91 p.

Manabe, S., and R.J. Stouffer (1994). Multiple-century response of a coupled ocean-atmosphere model to an increase of atmospheric carbon dioxide, J. Climate, 7, 5-23.

Marotzke, J., and B.A. Klinger (2000). The dynamics of equatorially asymmetric thermohaline circulations, J. Phys. Oceanogr., 30, 955-970.

Marzeion, B., A. Levermann and J. Mignot (2007). The role of stratification-dependent mixing for the stability of the Atlantic overturning in a global climate model, J. Phys. Oceanogr., *37*, 2672-2681.

Marzeion, B., A. Levermann and J. Mignot (2010). Sensitivity of North Atlantic subpolar gyre and overturning to stratification-dependent mixing: response to global warming, Clim. Dynam., *34*, 661-668.

Masina, S., P. Di Pietro, A. Storto and A. Navarra (2011). Global Ocean reanalyses for climate applications, Dynam. Atmos. Oceans, *52* (1), 341-366; doi:10.1016/j.dynatmoce.2011.03.006.

Meehl, G.A., et al. (2013). Climate change projections in CESM1 (CAM5) compared to CCSM4, J. Climate, *26*, 6287-6308; doi:10.1175/JCLI-D-12-00572.1.

Mikolajewicz, U., and R. Voss (2000). The role of the individual air-sea flux component in CO_2-induced changes of the ocean's circulation and climate, Clim. Dynam., *16*, 627-642.

Nilsson, J., and G. Walin (2001). Freshwater forcing as a booster of thermohaline circulation, Tellus A, *53* (5), 629-641.

Nilsson, J., G. Brostrom and G. Walin (2003). The thermohaline circulation and vertical mixing: Does weaker density stratification give stronger overturning?, J. Phys. Oceanogr., *33*, 2781-2795.

Rahmstorf, S. (2002). Ocean circulation and climate during the past 120,000 years, Nature, *419*, 207-214.

Reid, J.L. (1989). On the total geostrophic circulation of the South Atlantic Ocean: flow patterns, tracers and transports, Prog. Oceanogr., *23*, 149.

Roeckner, E., K. Arpe, L. Bengtsson, M. Christoph, M. Claussen, L. Dumenil, M. Esch, M. Giorgetta, U. Schelse and U. Schulzweida (1996). The Atmospheric general circulation Model ECHAM4: model description and simulation of present-day climate, Max Planck Institut für Meteorologie, Report no. 218, Hamburg, 86 p.

Saenko, O.A., and A.J. Weaver (2004). What drives heat transport in the Atlantic: Sensitivity to mechanical energy supply and buoyancy forcing in the Southern Ocean, Geophys. Res. Lett., *31*, L20305; doi:10.1029/2004GL020671.

Schmittner, A., M. Latif and B. Schneider (2005). Model projections of the North Atlantic thermohaline circulation for the 21st century assessed by observations, Geophys. Res. Lett., *32*, L23710; doi:10.1029/2005GL024368.

Sévellec, F., and A.V. Fedorov (2011). Stability of the Atlantic meridional overturning circulation and stratification in a zonally averaged ocean model: effects of freshwater, Southern ocean wind and diapycnal diffusion, Deep-Sea Res. Pt. II, *58*, 1927-1943; doi:10.1016/j.dsr2.2010.10.070.

Stocker, T.F., and A. Schmittner (1997). Influence of CO_2 emission rates on the stability of the thermohaline circulation, Nature, *388*, 862-865.

Stouffer, R.J., J. Yin, J.M. Gregory, K.W. Dixon, M.J. Spelman et al. (2006). Investigating the causes of the response of the thermohaline circulation to past and future climate changes, J. Climate, *19*, 698-722.

Thorpe, R.B., J.M. Gregory, T.C. Johns, R.A. Wood and J.F.B. Mitchell (2001). Mechanisms determining the Atlantic thermohaline circulation response to greenhouse gas forcing in a non-flux-adjusted coupled climate model, J. Climate, *14*, 3102-3116.

Timmermann, R., H. Goosse, G. Madec, T. Fichefet, C. Etheb and V. Duliére (2005). On the representation of high latitude processes in the ORCA-LIM global coupled sea ice-ocean model, Ocean Model., *8*, 175-201.

Toggweiler, J.R., and B. Samuels (1995). Effect of Drake passage on the global thermohaline circulation, Deep-Sea Res. Pt. I, *42*, 477-500.

Toggweiler, J.R. (2009). Shifting Westerlies, Science, *323*, 1434-1435.

Unesco (1981). The Practical Salinity Scale 1978 and the International Equation of State of Sea water 1980, Unesco technical papers in marine science, *36* , *25* p.

Valcke, S., L. Terray and A. Piacentini (2000). The Oasis coupler user guide version 2.4, Tech. Rep. TR/CM GC/00-10, CERFACS.

Weaver, A.J., M. Eby, M. Kienast and O.A. Saenko (2007). Response of the Atlantic meridional overturning circulation to increasing atmospheric CO_2: sensitivity to mean climate state, Geophys. Res. Lett., *34*, L05708; doi:10.1029/2006GL028756.

Welander, P. (1986). Thermohaline effects in the ocean circulation and related simple models, In: J. Willebrand and D.L.T. Anderson (eds.), Large scale transport processes in the oceans and atmosphere, D. Reidel Publishing Company, 163-200.

Wood, R., A.A.B. Keen, J.F.B. Mitchell and J.M. Gregory (1999). Changing spatial structure of the thermohaline circulation in response to atmospheric CO_2 forcing in a climate model, Nature, *399*, 572-575.

*Corresponding author: Rita Lecci,
Fondazione Centro Euro-Mediterraneo sui Cambiamenti Climatici, Lecce, Italy; email: rita.lecci@cmcc.it.